Composites Part B 134 (2018) 177–185

Contents lists available at ScienceDirect

Composites Part B

journal homepage: www.elsevier.com/locate/compositesb

Understanding the increase of the electric permittivity of cement caused by latex addition

Min Wang [1], D.D.L. Chung [*]

Composite Materials Research Laboratory, Department of Mechanical and Aerospace Engineering, University at Buffalo, The State University of New York, Buffalo, NY 14260-4400, USA

ARTICLE INFO

Article history:
Received 24 April 2017
Received in revised form
27 September 2017
Accepted 28 September 2017
Available online 29 September 2017

Keywords:
Ceramic-matrix composites (CMCs)
Particle-reinforcement
Electrical properties
Permittivity

ABSTRACT

The addition to cement paste of latex (styrene-butadiene, latex/cement mass ratio ≤0.30, where latex refers to the latex dispersion with 48 wt.% latex solid) increases the relative permittivity (2 kHz) from 27 to 43. The permittivity increases abruptly at latex/cement ratio ≤0.05, levels off at ratio 0.2, and increases abruptly at ratio ≥0.25. The increase occurs in spite of the low permittivity of latex solid compared to cement. It is attributed to the interface between cement and latex solid. The permittivity is modeled as the cement, latex solid and latex-cement interface in parallel electrically. Cement is the main contributor, followed by the latex-cement interface.

1. Introduction

The electric permittivity (the real part of the complex permittivity, also known as the dielectric constant) is a material property that pertains to the piezoelectric, dielectric and electric polarization behavior. The piezoelectric behavior of cement-based materials relates to the use of these materials as sensors and actuators [1–4]. The permittivity is one of the key material properties that govern the interaction of electromagnetic radiation with a material. Such interaction pertains to the probing of concrete with ground-penetrating radar [5] and the use of concrete for electromagnetic interference (EMI) shielding [6–8]. The polarization behavior affects the use of the electrical conductivity of these materials, since the polarization results in a reverse electric field in the material [9,10]. The polarization is also affected by stress, thus allowing polarization-based stress sensing [11]. The electrical conduction behavior of cement-based materials relates to the use of these materials in piezoresistivity-based strain/damage sensing [12–15], anti-static components [16], resistance-heating-based deicing [17,18], electrical grounding, and lightning protection. The conduction behavior is also relevant to the cathodic protection of the steel embedded in concrete [19–22] and to the removal of ions from these materials by electrochemical processes [22]. In spite of the relevance to numerous applications, the electric permittivity of cement-based materials has received little prior attention [23–25]. Most prior work on the permittivity of cement-based materials concerns the process of hydration [26–29].

Latex-modified cement-based materials are attractive for their enhanced flexural strength [30–32], flexural toughness [32] and vibration damping ability [33], decreased average crack width [34], reduced void content [32], and improved adhesion and bonding properties [35–37]. However, the electrical behaviors of these materials have received little prior attention [32]. It has been reported that latex addition to cement increases both the electrical resistivity [32] and the electric permittivity [23]. The increase in resistivity is expected, since latex (a polymer) is an electrical insulator, while cement is conductive. However, the increase in electric permittivity is not expected, since the permittivity of latex (as typical for polymers) is lower than that of cement. No explanation for the increase in permittivity by latex addition has been provided by the prior work. However, it is reasonable to conjecture that polarization occurs at the interface between latex and cement, thereby causing the permittivity to be increased by the latex addition.

* Corresponding author.
E-mail address: ddlchung@buffalo.edu (D.D.L. Chung).
URL: http://alum.mit.edu/www/ddlchung

[1] Permanent address: The Key Laboratory of Space Applied Physics and Chemistry, Ministry of Education and Shaanxi Key Laboratory of Macromolecular Science and Technology, School of Science, Northwestern Polytechnical University, Xi'an 710072, PR China.

https://doi.org/10.1016/j.compositesb.2017.09.068
1359-8368/

Latex is most commonly used as an admixture in cement. However, latex has also been used as a protective coating on glass fiber fabric that is used to reinforce cement [38]. Polymer fibers such as polypropylene fibers are also used admixtures in cement to improve the toughness [39]. The combined use of polymer fiber and latex as admixtures is attractive for controlling the multiple cracking behavior [40].

This paper is aimed at (i) understanding the effect of latex addition on the electric permittivity of cement, (ii) modeling the electric permittivity based on the contributions of the constituents (namely cement, latex and cement-latex interface) to the permittivity of latex-modified cement, (iii) investigating the effect of the latex/cement ratio on each of these contributions, and (iv) advancing the science related to the permittivity of cement-based materials.

2. Experimental methods

2.1. Materials

Portland cement (Type I, ASTM C150) from Lafarge (Southfield, MI) is used. No aggregate is used. The water/cement mass ratio is fixed at 0.45, with the water including that in the latex dispersion. The latex dispersion (#460NA, Dow Chemical, Midland, MI) has a styrene butadiene copolymer with the polymer making up 48% of the dispersion mass and with the styrene and butadiene having a mass ratio of 66:34. An antifoaming agent (#2410, Dow Corning, Midland, MI) is used. The antifoam content is fixed at 0.5% by mass of latex dispersion. All the ingredients are mixed in a rotary mixer with a flat beater. The mix proportions are shown in Table 1.

Firstly, the latex dispersion is mixed with the antifoam by hand for about 1 min. Secondly, the latex dispersion and water are mixed for 2 min. Then, the resulting mixture is added to the cement and stirred for 5 min. Then the mixture is poured into an oiled mold of dimensions 25 mm × 25 mm. The specimens are demolded after 1 day and cured in air at room temperature (relative humidity = 100%) for the next 27 days. Before capacitance measurement, the samples are burnished to ensure that the surfaces are smooth. Various values of the specimen thickness are used, as described in Table 2. All three dimensions are separately measured for each specimen.

2.2. Permittivity measurement and analysis method

The permittivity is measured using the parallel-plate capacitor geometry, with two electrical contacts sandwiching the specimen symmetrically. An electrical contact (copper foil of thickness 0.15 mm) covers the entire area of each of the two square surfaces of the specimen. Between each of the two copper foils and the specimen is positioned a dielectric Teflon-coated glass fiber composite film (thickness 58 μm, relative permittivity 1.5 at 2 kHz). This dielectric film is used because the RLC meter used for the capacitance measurement is not designed to measure the capacitance of a conductive material. Cement-based materials without conductive admixtures are not conductive enough for the dielectric film to be necessary. Nevertheless, the film is used in this work. A pressure of 9.93 kPa is applied in the direction perpendicular to the plane of the sandwich.

The capacitance is measured using a precision LCR meter (Instek LCR-816 High Precision LCR Meter, 100 Hz-2 kHz), with the electric field across the thickness of the specimen fixed at 0.10 V/mm. The voltage is increased with the specimen thicknesses; for example, for a specimen thickness of 3.90 mm, the voltage is 0.39 V. The frequency used is 2 kHz. The capacitance reported here is that for the equivalent electrical circuit of a capacitance and a resistance in parallel.

The methodology for measuring the capacitance involves firstly the separation of the interfacial capacitance (interface between the specimen and an electrical contact) from the volumetric capacitance (the volume of the specimen). This decoupling is enabled by the testing of three different thicknesses of the sandwiched specimen and plotting the inverse of the measured capacitance C_m vs. thickness l (Fig. 1). The slope of the straight-line plot is equal to $1/(\kappa\varepsilon_o A)$, where κ is the relative permittivity of the specimen, ε_o is the permittivity of free space, and A is the area of the sandwiched dielectric material. Hence, κ is obtained from the reciprocal of the slope. The intercept of the straight with the vertical axis at zero thickness equals $2/C_i$, where C_i is the capacitance of one interface. In other words,

$$1/C_m = 1/C_v + 2/C_i, \tag{1}$$

where C_v is the volumetric capacitance. Using Eq. (1), which is based on capacitors in series, $1/C_v$ is obtained for a given value of l. The C_v is given by

$$C_v = \varepsilon_o\ \kappa\ A/l, \tag{2}$$

where ε_o is the permittivity of free space (8.85×10^{-12} F/m), A is the area of the sandwich (i.e., the area of the electrical contact), and l is the thickness of the specimen sandwiched by the electrical contacts.

The cement, latex solid and the interface between these components are modeled electrically as continuous dielectric components that are either in parallel or in series, with capacitances C_C, C_L and C_I, respectively. Water is included in the cement component. In addition, moisture may be present at the interface between cement and latex solid. The effect of the amount of water is not addressed in this paper, as the water/cement ratio is fixed.

With the cement and latex solid components alternating in their positions (Fig. 2), let N be the number of cement layers. Then the number of latex solid layer is $N-1$ and the number of interfaces is $2N-2$. The effect of the degree of dispersion of the latex is not addressed in this paper, as the mixing condition is fixed.

In the parallel model (Fig. 2(a)), according to the Rule of Mixtures [41],

$$C_v = NC_C + (N-1)C_L + (2N-2)C_I. \tag{3}$$

Rearrangement gives the contribution of the interfaces to the relative permittivity of the cement-based material as

$$(2N-2)\frac{C_I\, l}{A\varepsilon_0} = \kappa - V_C\kappa_C - V_L\kappa_L, \tag{4}$$

where V_C and κ_C are the volume fraction and relative permittivity of cement, respectively, and V_L and κ_L are is the volume fraction and

Table 1
Mix proportions for the cement-based materials studied.

Latex[a]/cement mass ratio	Cement (g)	Latex[a] (g)	Water (g)	Antifoam (g)
0	100.0 ± 0.5	0	45.0 ± 0.05	0
0.05	100.0 ± 0.5	5.0 ± 0.5	42.4 ± 0.05	0.025
0.10	100.0 ± 0.5	10.0 ± 0.5	39.8 ± 0.05	0.050
0.15	100.0 ± 0.5	15.0 ± 0.5	37.2 ± 0.05	0.075
0.20	100.0 ± 0.5	20.0 ± 0.5	34.6 ± 0.05	0.100
0.25	100.0 ± 0.5	25.0 ± 0.5	32.0 ± 0.05	0.125
0.30	100.0 ± 0.5	30.0 ± 0.5	29.4 ± 0.05	0.150

[a] Latex dispersion.

Table 2
The measured capacitance C_m and the relative permittivity κ obtained from the slope of the plot of $1/C_m$ vs. thickness l.

Latex[a]/cement mass ratio	Cement volume fraction	Latex solid volume fraction	Thickness (mm)	Area (mm^2)	C_m (pF)	κ
0	1.00	0	1.91	25.04 × 24.60	22.44 ± 0.01	26.98 ± 0.90
			3.28	23.89 × 24.66	19.20 ± 0.04	
			3.90	24.86 × 24.94	17.13 ± 0.02	
0.05	0.96 ± 0.01	0.038 ± 0.000	1.33	24.36 × 24.30	21.17 ± 0.01	32.87 ± 0.77
			2.71	24.38 × 24.47	18.37 ± 0.02	
			3.52	25.03 × 25.28	16.84 ± 0.01	
0.10	0.93 ± 0.01	0.072 ± 0.000	1.99	25.38 × 25.24	20.64 ± 0.01	36.16 ± 0.60
			2.74	25.11 × 24.96	19.04 ± 0.05	
			3.39	25.42 × 25.05	18.04 ± 0.04	
0.15	0.89 ± 0.01	0.10 ± 0.00	1.86	25.17 × 25.07	18.74 ± 0.01	37.66 ± 0.82
			2.38	22.43 × 23.88	17.91 ± 0.03	
			3.28	23.99 × 24.46	16.63 ± 0.02	
0.20	0.86 ± 0.01	0.14 ± 0.00	1.85	25.19 × 24.88	17.13 ± 0.01	39.30 ± 0.60
			2.39	25.10 × 25.35	16.51 ± 0.05	
			3.51	25.02 × 24.94	15.18 ± 0.03	
0.25	0.84 ± 0.01	0.16 ± 0.00	1.72	24.88 × 24.88	20.22 ± 0.03	40.18 ± 0.53
			2.50	24.85 × 24.89	18.97 ± 0.02	
			3.02	25.24 × 25.11	18.05 ± 0.02	
0.30	0.81 ± 0.01	0.19 ± 0.00	1.35	24.69 × 24.53	21.60 ± 0.01	43.04 ± 0.32
			2.40	24.88 × 24.38	19.74 ± 0.02	
			3.12	24.78 × 24.80	18.60 ± 0.04	

[a] Latex dispersion.

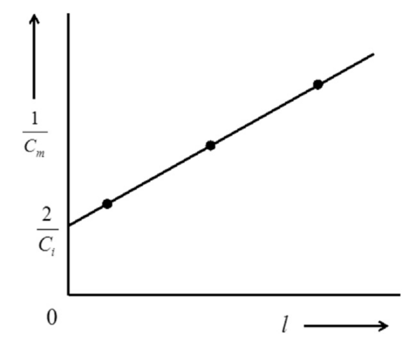

Fig. 1. Schematic plot of $1/C_m$ vs. l, for the determination of C_i and κ based on Eq. (1), where C_m is the measured capacitance, C_i is the capacitance of a specimen-contact interface, l is the thickness of the specimen, and κ is the relative permittivity of the specimen. The slope equals $1/(\varepsilon_o \kappa A)$, where A is the area of the specimen. The intercept on the vertical axis equals $2/C_i$.

relative permittivity of latex solid, respectively. The terms $V_C\kappa_C$ and $V_L\kappa_L$ are the contributions of the cement and latex solid to the relative permittivity of the cement-based material, respectively. The volume fractions are obtained from the mass fractions (Table 1, with the fraction of solid in the latex dispersion taken into consideration) and the densities. The density of cement is taken as 1.62 g/cm^3, which is the density of the cement-based material without latex addition, as measured in this work. The density of latex solid (with 66% styrene) is taken as 0.994 g/cm^3, which is obtained by extrapolating the known densities of styrene-butadiene of 0.965 g/cm^3 at 45% styrene and 0.910 g/cm^3 for 5% styrene [42]. The relative permittivity of styrene-butadiene solid is 2.8 [43].

In the series model (Fig. 2(b)), according to the Rule of Mixtures [41],

$$1/C_v = N/C_C + (N - 1)/C_L + (2N - 2)/C_I. \quad (5)$$

Rearrangement of Eq. (5) gives the contribution of the interfaces to the reciprocal of the relative permittivity of the cement-based material as

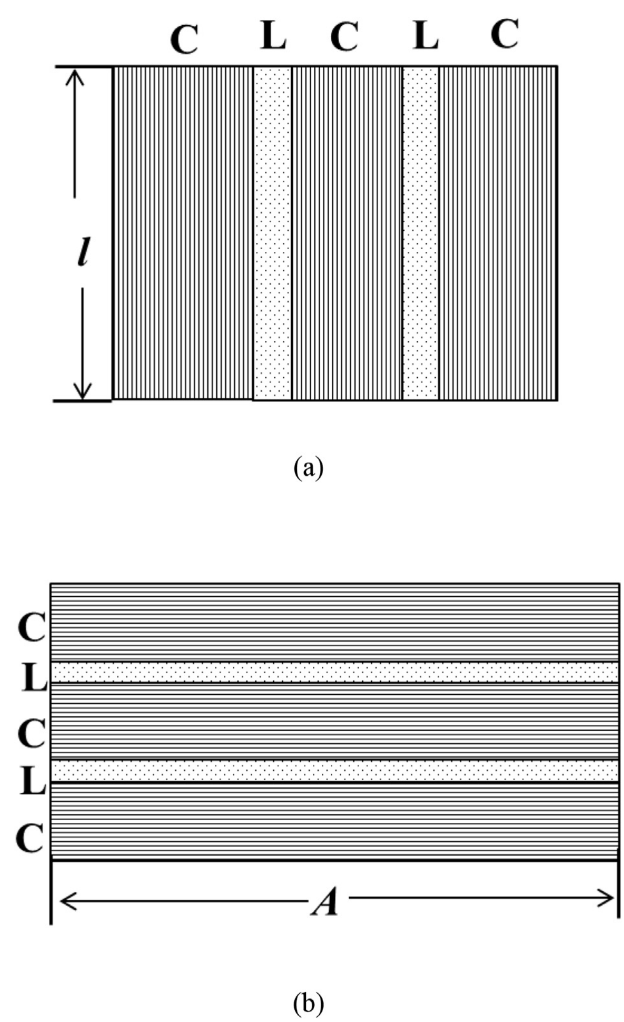

Fig. 2. Equivalent electric circuit models for the cement-based materials of this work. **C** = cement; **L** = latex solid. (a) The parallel model. (b) The series model.

$$(2N - 2)\frac{A\varepsilon_0}{C_I\, l} = 1/\kappa - V_C/\kappa_C - V_L/\kappa_L. \quad (6)$$

The terms V_C/κ_C and V_L/κ_L are the contributions of the cement and latex solid to the reciprocal of the relative permittivity of the cement-based material, respectively.

3. Results and discussion

Fig. 3 shows that the experimental plot of $1/C_m$ vs. l is indeed linear, as observed for all of the cement-based materials studied and as illustrated schematically in Fig. 1. Table 3 shows that the relative permittivity κ of the cement-based material increases monotonically with increasing latex/cement ratio. The value is increased from 27 to 43 when the latex/cement ratio is increased from 0 to 0.30.

The closest prior work [23] reported that the values of the relative permittivity at 10 kHz for cement pastes with latex/cement ratios 0 and 0.2 are 29 and 35, respectively. In spite of the difference in frequency, at the same latex/cement ratio, the permittivity is only slightly lower in the present work than the prior work [23]. This difference is attributed to the fact that the prior work uses a single specimen thickness in determining the permittivity from the capacitance, whereas the present work uses three specimen thicknesses for determining the permittivity from the slope of the plot of the inverse capacitance vs. thickness. Thus, the prior work does not decouple between the capacitance from the specimen-contact interface and the specimen capacitance, whereas the present work does. Without the decoupling, the inverse of the interfacial capacitance ($1/C_i$) is lumped in with the inverse of the specimen capacitance ($1/C_v$), in accordance with Eq. (1), so that the inverse of the specimen capacitance is over-estimated. This over-estimation means that the specimen capacitance is under-estimated. As a consequence, κ is also underestimated. The lower value of κ in the prior work [23] is probably also due to the higher frequency used.

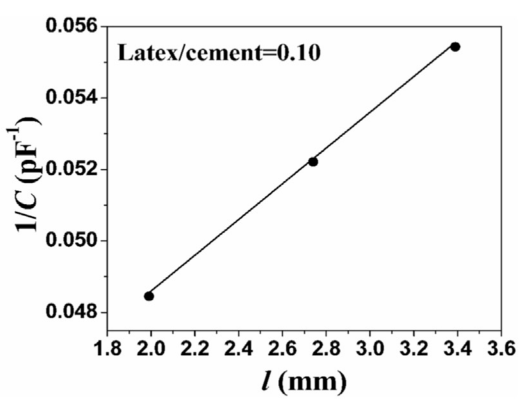

(a)

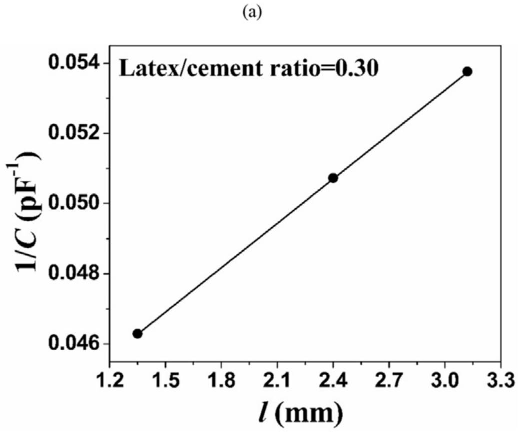

(b)

Fig. 3. Representative plots of $1/C_m$ versus l, where C_m is the measured capacitance and l is the specimen thickness, as shown for (a) latex/cement ratio = 0.10, and (b) latex/cement = 0.30.

For the parallel model, Table 3 shows that the cement is the main contributor to the relative permittivity of the cement-based material. This is expected from the high proportion of cement in the mix (Table 1). The contribution from the latex solid is small, as expected from the low proportion of latex dispersion in the mix (Table 1). The contribution from the interface between cement and latex solid is substantial, though it is below that of the cement. As the latex/cement ratio increases, the contributions from the latex solid and from the cement-latex increase, while that from the cement decreases. As a consequence, at a high latex/cement ratio (such as 0.30), the contribution from the cement-latex interface approaches that from the cement. Therefore, the increase in the relative permittivity of the cement-based material with increasing latex/cement ratio is mainly due to the cement-latex interface.

For the series model, Table 4 shows that the cement and latex solid contribute positively to the reciprocal of the relative permittivity of the cement-based material, while the cement-latex interface contributes negatively. This suggests polarization in the reverse direction at the cement-latex interface. The cement is the main contributor to the reciprocal of the relative permittivity when the latex/cement ratio is 0.10 or below, with the latex solid being the smallest contributor. At higher values of the latex/cement ratio, the cement is the smallest contributor, while the cement-latex interface is the greatest contributor (though negative). The contribution from the latex solid and that from the interface increase with increasing latex/cement ratio, while that from the cement decreases. Therefore, the decrease of the reciprocal of the relative permittivity (i.e., the increase of the relative permittivity) with increasing latex/cement ratio is mainly due to the cement-latex interface.

Although the results of the series model are not totally unreasonable, the high negative values of the contribution from the cement-latex interface is not likely to be feasible, as there is no reasonable mechanism that would enable this. Therefore, the parallel model (Table 3) is much closer to reality that the series model (Table 4).

As shown in Fig. 4, the relative permittivity κ of the cement-based material increases with the latex/cement ratio (where the latex refers to the latex dispersion). It increases abruptly at a low latex/cement ratio of $\leq$0.05, levels off at a ratio of about 0.2, and increases abruptly at a ratio $\geq$0.25. The abrupt increase at a ratio $\geq$0.25 is attributed to the dielectric percolation of the latex solid phase, which leads to the dielectric percolation of the interface between latex solid and cement. The abrupt increase at ratio $\leq$0.05 is attributed to the introduction of the interface when the latex content is increased from zero. The shape of the curve in Fig. 4 is in contrast to the roughly linear increase of the electrical resistivity with the latex/cement ratio [32]. The increase of the resistivity with latex content is due to the high resistivity of latex solid compared to cement. However, the increase in the relative permittivity with increasing latex content is mainly due to the increasing abundance of the interface between cement and latex solid. In addition, conduction percolation and dielectric percolation are not the same, as the former involves charge carrier movement whereas the latter involves polarization.

As shown in Fig. 5, according to the parallel model, the

Table 3
The relative permittivity κ of the cement-based materials and the contributions to κ from the constituents, based on the parallel model and Eq. (4). The constituents are cement, latex solid and the interface between cement and latex solid, with these contributions given respectively by $V_C\, \kappa_C$, $V_L\, \kappa_L$ and $(2N - 2)\, C_I\, l/(A\varepsilon_0)$.

Latex[a]/cement mass ratio	κ	Contributions to κ by the constituents, based on the parallel model		
		Cement	Latex solid	Cement-latex interface
0	26.98 ± 0.90	26.98 ± 0.90	0	0
0.05	32.87 ± 0.77	25.96 ± 0.24	0.100 ± 0.004	6.80 ± 0.78
0.10	36.16 ± 0.60	25.02 ± 0.25	0.200 ± 0.007	10.93 ± 0.61
0.15	37.66 ± 0.82	24.15 ± 0.22	0.290 ± 0.010	13.22 ± 0.82
0.20	39.30 ± 0.60	23.33 ± 0.19	0.380 ± 0.012	15.59 ± 0.60
0.25	40.18 ± 0.53	22.57 ± 0.18	0.460 ± 0.016	17.15 ± 0.32
0.30	43.04 ± 0.32	21.85 ± 0.17	0.530 ± 0.019	20.66 ± 0.91

[a] Latex dispersion.

Table 4
Contributions to $1/\kappa$ from the constituents, where κ is the relative permittivity of the cement-based material, based on the series model and Eq. (6). The constituents are cement, latex solid and the interface between cement and latex solid, with these contributions given respectively by V_C/κ_C, V_L/κ_L and $(2N - 2)\, A\varepsilon_0/(C_I\, l)$.

Latex[a]/cement mass ratio	$1/\kappa$ (10^{-2})	Contributions to $1/\kappa$ by the constituents, based on the series model (10^{-2})		
		Cement	Latex solid	Cement-latex interface
0	3.71 ± 0.07	3.71	0	0
0.05	3.04 ± 0.07	3.58 ± 0.02	1.22 ± 0.04	−1.76 ± 0.12
0.10	2.76 ± 0.07	3.46 ± 0.03	2.36 ± 0.08	−3.05 ± 0.13
0.15	2.66 ± 0.07	3.35 ± 0.03	3.42 ± 0.12	−4.12 ± 0.16
0.20	2.54 ± 0.06	3.25 ± 0.03	4.42 ± 0.16	−5.12 ± 0.19
0.20	2.49 ± 0.07	3.15 ± 0.02	5.36 ± 0.19	−6.02 ± 0.21
0.30	2.32 ± 0.07	3.06 ± 0.02	6.25 ± 0.22	−6.98 ± 0.25

[a] Latex dispersion.

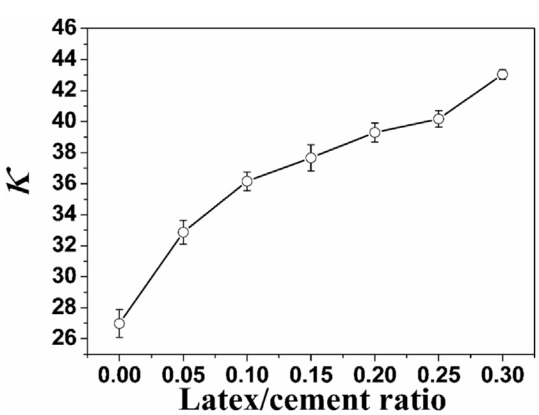

Fig. 4. Variation of the relative permittivity κ of the cement-based material with the latex/cement ratio, where the latex refers to the latex dispersion.

contribution of cement to the relative permittivity κ of the cement-based material decreases with the latex/cement ratio roughly linearly, whereas the contributions of latex solid and latex-cement interface increase with increasing latex/cement ratio. The increase of the contribution of the latex solid is roughly linear, but that of the contribution of the latex-cement ratio increases more abruptly at low and high values of the latex/cement ratio than the intermediate values, akin to the variation of κ with the latex-cement ratio (Fig. 4). The similarity in shape between the curves in Figs. 4 and 5(c) supports the notion that the increase in κ due to the increase in the latex-cement ratio is mainly due to the latex-cement interface.

According to the parallel model (Eq. (4)), the fractional contribution of the latex solid to the relative permittivity κ of the cement-based material (i.e., the contribution to κ from the latex solid as a fraction of κ) is given by

$\kappa_L V_L/\kappa$,

as shown in Fig. 6(a). The fractional contribution of the latex-cement interface to κ is given by

$(2N - 2)\, C_I\, l\, /\, (A\varepsilon_0\kappa)$,

as shown in Fig. 6(b). The fractional contribution of the latex solid to κ increases roughly linearly with increasing latex/cement ratio, such that it levels off at a latex/cement ratio ≥0.25. This is probably due to the percolation of latex solid at ratio ≥0.25. The fractional contribution of the latex-cement interface to κ increases relatively abruptly at low latex/cement ratio below 0.10 and at high ratio above 0.25. The shape of the curve in Fig. 6(b) is similar to that of the curve in Fig. 5(c) for the contribution of the latex-cement interface to κ, and is also similar to that of the curve in Fig. 4 for κ. This similarity is consistent with the notion that the latex-cement interface is mainly responsible for the increase of κ upon increase of the latex/cement ratio.

Fig. 7 shows that, for the series model, the contribution of the cement to the relative permittivity κ of the cement-based material decreases essentially linearly with increasing latex/cement ratio, whereas that of the latex solid increases essentially linearly, such that the increase becomes more gradual at a high latex/cement ratio of ≥0.20, probably due to latex solid percolation. The contribution from the latex-cement interface becomes increasingly negative as the latex/cement ratio increases, such that the dependence is essentially linear. None of the curves in Fig. 7 resemble the shape of Fig. 4. This lack of resemblance supports the notion that the series model is not effective.

For the series model (Eq. (6)), the fractional contribution from the latex solid to $1/\kappa$ is given by

$V_L\, \kappa/\kappa_L$,

as shown in Fig. 8(a), and the fractional contribution from the latex-cement interface to $1/\kappa$ is given by

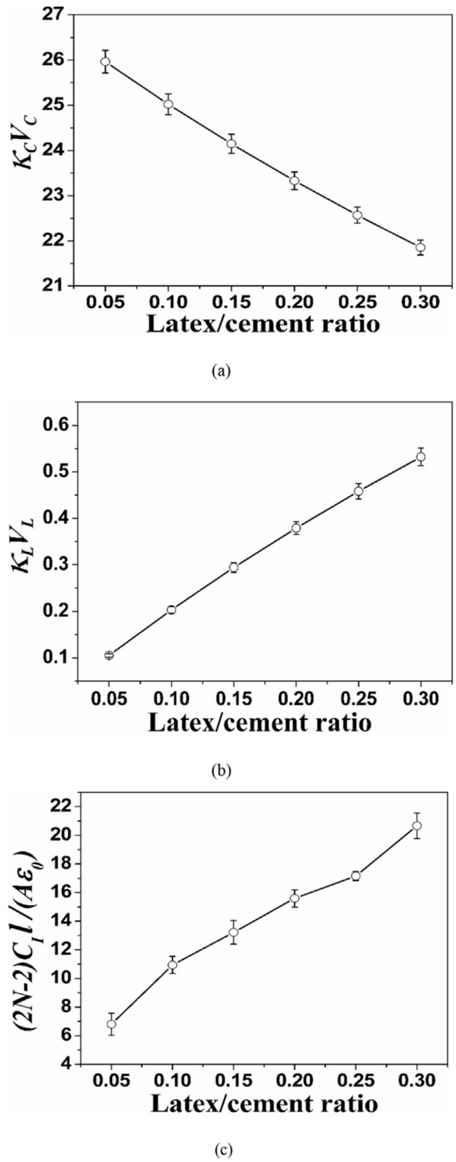

Fig. 5. Contributions of (a) the cement, (b) the latex solid and (c) the latex-cement interface, to the relative permittivity κ of the cement-based material, according to the parallel model.

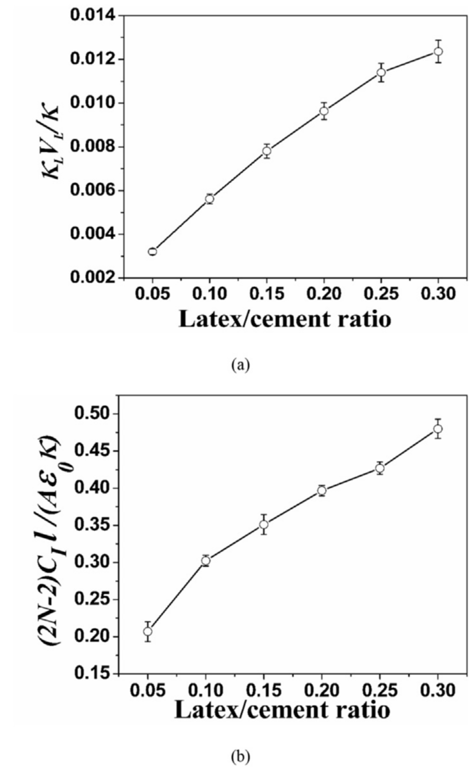

Fig. 6. The fractional contributions of (a) the latex solid and (b) the latex-cement interface, to the relative permittivity κ of the cement-based material as functions of the latex/cement ratio, according to the parallel model.

κ $(2N - 2)\, A\varepsilon_0/(C_I\, l)$.

The fractional contribution from the latex solid to $1/\kappa$ increases roughly linearly with increasing latex/cement ratio, such that the increase becomes more abrupt at a high latex/cement ratio $\geq$0.25. The fractional contribution from the latex-cement interface to $1/\kappa$ becomes increasingly negative (roughly linearly) with increasing latex/cement ratio, such that increase is more abrupt at a high latex/cement ratio $\geq$0.25. The greater abruptness at a high latex/cement ratio $\geq$0.25 is not consistent with the notion of percolation being expected to occur at high values of this ratio. In addition, the shapes of the curves in Fig. 8 do not resemble that of Fig. 4. Therefore, Fig. 8 supports the notion that the series model is not sufficiently effective.

Fig. 9 shows the equivalent circuit model that embodies the parallel model mentioned above. In this model, cement, latex solid and latex-cement interface are three circuit elements that are in parallel electrically. Each element is modeled as a resistance and a capacitance in parallel, though this paper addresses only the capacitance and not the resistance. This parallel combination is in series with two circuit elements that represent the two electrical contacts that sandwich the specimen. Hence, the model reflects the testing configuration.

A model that involves both parallel and series configurations is also possible. However, simplicity in the model is preferred. Therefore, the model of Fig. 9 is recommended.

The model of Fig. 9 implies a degree of continuity of the latex solid in cement-based material. The formation of latex film or network in cement has been previously reported, based on microstructural observations [44–47]. Moreover, the formation in cement of latex films penetrated by cement hydration products has also been reported [48]. Furthermore, the formation of latex in the form of particulate single-layers adsorbed on cement particles has been reported [49]. In addition, the presence of latex particles in cement has been observed [50]. Most commonly, latex addition has been reported to decrease the porosity [51,52], downshift the pore-size distribution [51,53] and reduce the water absorption [52].

The model of Fig. 9 also implies a degree of continuity of the latex-cement interface. This is supported by the previously reported formation of latex in the form of particulate single-layers adsorbed on cement particles [49]. It is also supported by the reported adsorption of the latex particles on the cement particles shortly after mixing [54].

This work uses a technique that differs greatly from the widely used technique of impedance spectroscopy, which measures the impedance as a function of frequency and uses the frequency dependence to obtain information. Firstly, the technique of this work does not measure the impedance, but measures the relative permittivity (real part of the permittivity). Secondly, the technique of this work decouples the contribution of the specimen-contact

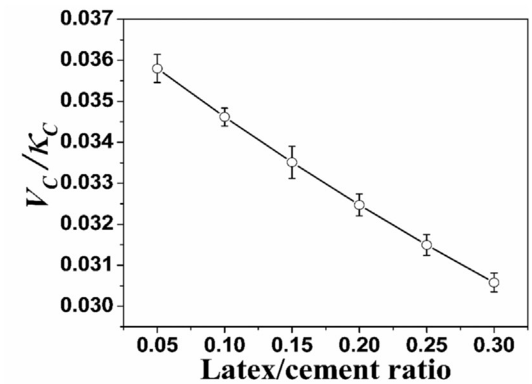

(a)

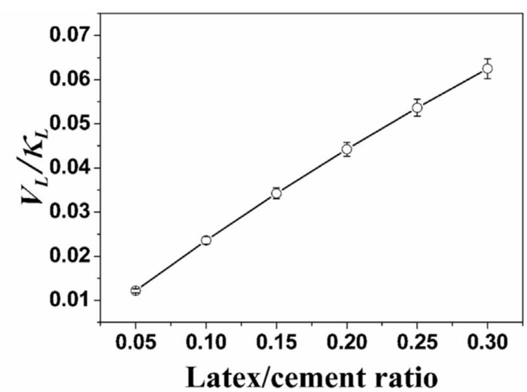

(b)

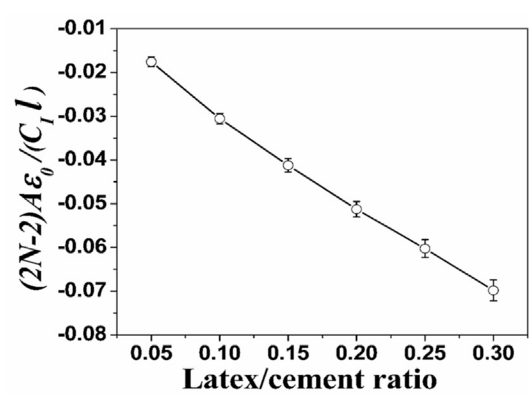

(c)

Fig. 7. Contributions of (a) the cement, (b) the latex solid and (c) the latex-cement interface to $1/\kappa$, where κ is the relative permittivity of the cement-based material, as functions of the latex/cement ratio, according to the series model.

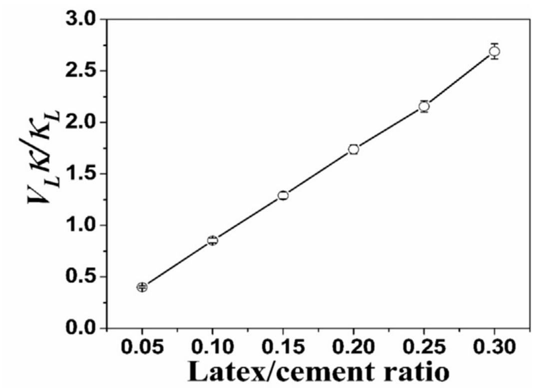

(a)

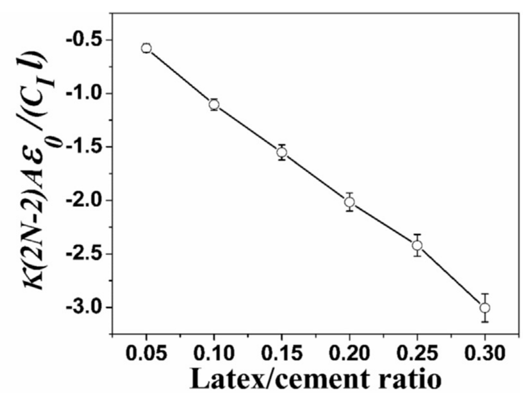

(b)

Fig. 8. The fractional contributions of (a) the latex solid and (b) the latex-cement interface, to $1/\kappa$, where κ is the relative permittivity of the cement-based material, as functions of the latex/cement ratio, according to the series model.

interface from the contribution of the volume of the specimen. This decoupling is not performed in impedance spectroscopy. Thirdly, the technique of this work uses an equivalent circuit model (Fig. 9) that reflects the testing configuration and material structure. Fourthly, the technique of this work does not need to address the frequency dependence in order to obtain meaningful information. In contrast, impedance spectroscopy is focused on the frequency dependence of the impedance, as conventionally described in terms of the Nyquist plot, for the purpose of deriving by mathematical fitting of the plot an equivalent electrical circuit that is intended to describe the electrical/dielectric behavior of the material. The circuit model obtained by the curve fitting tends to be not unique, so the determined values of the circuit elements in the model are not very meaningful.

4. Conclusions

Latex (styrene-butadiene copolymer) is the most commonly used polymer admixture in cement-based materials. This work strengthens the science of latex-modified cement by addressing the effect of latex addition on the electric permittivity. Most notably, this work shows that the interface between cement and latex solid contributes substantially to the permittivity of the latex-modified cement.

The addition to cement paste of latex up to a latex/cement mass ratio of 0.3 (with the latex in this ratio referring to the latex dispersion rather than the latex solid) increases the relative permittivity at 2 kHz from 27 to 43 when the latex/cement ratio is increased from 0 to 0.3. The permittivity increases abruptly at a low latex/cement ratio of $\leq$0.05, levels off at a ratio of about 0.2, and increases abruptly at a ratio $\geq$0.25. The increase occurs in spite of the low permittivity of latex solid compared to cement. It is attributed to the contribution to the permittivity from the interface between the cement and latex solid.

The permittivity of the cement-based material is effectively modeled by considering cement, latex solid and the latex-cement interface as three continuous constituents in parallel electrically. The series model is not effective. The cement is the main

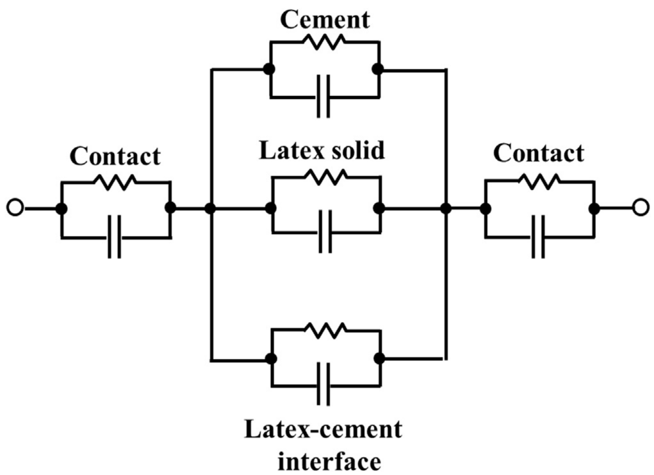

Fig. 9. Equivalent circuit model (parallel model) for the electrical behavior of latex-modified cement. The contact refers to the interface between the specimen and an electrical contact.

contributor to the relative permittivity. The contribution from the latex solid is small. The contribution from the interface between cement and latex solid is substantial, though it is below that of the cement. As the latex/cement ratio increases, the contributions from the latex solid and from the cement-latex increase, while that from the cement decreases. As a consequence, at a high latex/cement ratio (such as 0.30), the contribution from the cement-latex interface approaches that from the cement. The contribution of cement to the relative permittivity κ of the cement-based material decreases with the latex/cement ratio roughly linearly, whereas the contributions of latex solid and latex-cement interface increase with increasing latex/cement ratio. The increase of the contribution of the latex solid is roughly linear, but that of the contribution of the latex-cement ratio increases more abruptly at low and high values of the latex/cement ratio than the intermediate values, akin to the variation of κ with the latex-cement ratio. This similarity is consistent with the notion that the latex-cement interface is mainly responsible for the increase of κ upon increase of the latex/cement ratio.

The fractional contribution of the latex solid (i.e., the contribution to κ from the latex solid as a fraction of κ) increases roughly linearly with increasing latex/cement ratio, such that it levels off at a latex/cement ratio $\geq$0.25, probably due to the percolation of latex solid at ratio $\geq$0.25. The fractional contribution of the latex-cement interface increases relatively abruptly at low latex/cement ratio below 0.10 and at high ratio above 0.25.

References

[1] Ramam K, Chandramouli K. Piezoelectric cement composite for structural health monitoring. Adv Cem Res 2012;24:165–71.
[2] Shen B, Yang X, Li Z. A cement-based piezoelectric sensor for civil engineering structure. Mater Struct Dordr Neth 2006;39:37–42.
[3] Lam KH, Chan HLW. Piezoelectric cement-based 1-3 composites. Appl Phys A 2005;81:1451–4.
[4] Zhang D, Li Z, Wu K. 2-2 Piezoelectric cement matrix composite: Part II. Actuator effect. Cem Concr Res 2002;32:825–30.
[5] Van Den Bril K, Gregoire C, Swennen R, Lambot S. Ground-penetrating radar as a tool to detect rock heterogeneities (channels, cemented layers and fractures) in the Luxembourg Sandstone Formation (Grand-Duchy of Luxembourg). Sedimentology 2007;54:949–67.
[6] Muthusamy S, Chung DDL. Carbon fiber cement-based materials for electromagnetic interference shielding. ACI Mater J 2010;107:602–10.
[7] Cao J, Chung DDL. Use of fly ash as an admixture for electromagnetic interference shielding. Cem Concr Res 2004;34:1889–92.
[8] Wen S, Chung DDL. Electromagnetic interference shielding reaching 70 dB in steel fiber cement. Cem Concr Res 2004;34:329–32.
[9] Cao J, Chung DDL. Electric polarization and depolarization in cement-based materials, studied by apparent electrical resistance measurement. Cem Concr Res 2004;34:481–5.
[10] Wen S, Chung DDL. Electric polarization in carbon fiber reinforced cement. Cem Concr Res 2001;31:141–7.
[11] Wen S, Chung DDL. Effect of stress on the electric polarization in cement. Cem Concr Res 2001;31:291–5.
[12] Wen S, Chung DDL. Piezoresistivity-based strain sensing in carbon fiber reinforced cement. ACI Mater J 2007;104:171–9.
[13] Zhu S, Chung DDL. Theory of piezoresistivity for strain sensing in carbon fiber reinforced cement under flexure. J Mater Sci 2007;42:6222–33.
[14] Wen S, Chung DDL. A comparative study of steel- and carbon-fiber cement as piezoresistive strain sensors. Adv Cem Res 2003;15:119–28.
[15] Chung DDL. Piezoresistive cement-based materials for strain sensing. J Intel Mat Syst Str 2002;13:599–609.
[16] Shalaby A, Ward A, Refaee A, Abd-El-Messieh S, Abd-El-Nour K, El-Nashar D, et al. Compressive strength and electrical properties of cement paste utilizing waste polyethylene terephthalate bottles. J Appl Sci Ress 2013;9:4160–73.
[17] Chang C, Ho M, Song G, Mo Y, Li H. A feasibility study of self-heating concrete utilizing carbon nanofiber heating elements. Smart Mater Struct 2009;18. 127001/1–127001/5.
[18] Wang S, Wen S, Chung DDL. Resistance heating using electrically conductive cements. Adv Cem Res 161–166.
[19] Hou J, Chung DDL. Cathodic protection of steel reinforced concrete facilitated by using carbon fiber reinforced mortar or concrete. Cem Concr Res 1997;27: 649–56.
[20] Aperador W, Bautista-Ruiz J, Chunga K. Determination of the efficiency of cathodic protection applied to alternative concrete subjected to carbonation and chloride attack. Int J Electrochem 2015;10:7073–82.
[21] Jeong J. Cathodic prevention and cathodic protection of concrete slab with zinc sacrificial anode. Appl MechMater 2014;597:341–4.
[22] Carmona J, Garces P, Climent MA. Efficiency of a conductive cement-based anodic system for the application of cathodic protection, cathodic prevention and electrochemical chloride extraction to control corrosion in reinforced concrete structures. Corros Sci 2015;96:102–11.
[23] Wen S, Chung DDL. Effect of admixtures on the dielectric constant of cement paste. Cem Concr Res 2001;31:673–7.
[24] Wang Y, Chung DDL. Effect of the fringing electric field on the apparent electric permittivity of cement-based materials. Compos part b 2017;126: 192–201.
[25] Sachdev VK, Sharma SK, Bhattacharya S, Patel K, Mehra NC, Gupta V, et al. Electromagnetic shielding performance of graphite in cement matrix for applied application. Adv Mater Lett 2015;6:965–72.
[26] Makul N. Dielectric permittivity of various cement-based materials during the first 24 hours hydration. Open J Inorg Non-Metallic Mater 2013;3:53–7.
[27] Simon D, Grabinsky MW. Electromagnetic wave-based measurement techniques to study the role of Portland cement hydration in cemented paste backfill materials. Int J Min Reclam Env 2012;26:3–28.
[28] Tsonos C, Stavrakas I, Anastasiadis C, Kyriazopoulos A, Kanapitsas A, Triantis D. Probing the microstructure of cement mortars through dielectric parameters' variation. J Phys Chem Solids 2009;70:576–83.
[29] Abe Y, Asano M, Kita R, Shinyashiki N, Yagihara S. Dielectric study on molecular dynamics in cement hydration. Trans Mater Res Soc Jpn 2008;33: 447–50.
[30] Benali Y, Ghomari F. Latex influence on the mechanical behavior and durability of cementitious materials. J Adhes Sci Technol 2017;31:219–41.
[31] Zhong S, Chen Z. Properties of latex blends and its modified cement mortars. Cem Concr Res 2002;32:1515–24.
[32] Fu X, Chung DDL. Degree of dispersion of latex particles in cement paste, as assessed by electrical resistivity measurement. Cem Concr Res 1996;26(7): 985–91.
[33] Fu X, Chung DDL. Vibration damping admixtures for cement. Cem Concr Res 1996;26:69–75.
[34] Ramli M, Tabassi AA. Mechanical behavior of polymer-modified ferrocement under different exposure conditions: an experimental study. Compos part b 2012;43:447–56.
[35] Fu X, Chung DDL. Effect of polymer admixtures to cement on the bond strength and electrical contact resistivity between steel fiber and cement. Cem Concr Res 1996;26:189–94.
[36] Fu X, Chung DDL. Effects of water-cement ratio, curing age, silica fume, polymer admixtures, steel surface treatments, and corrosion on bond between concrete and steel reinforcing bars. ACI Mater J 1998;95:725–34.
[37] Issa CA, Assaad JJ. Stability and bond properties of polymer-modified self-consolidating concrete for repair applications. Mater Struct Dordr Neth 2017;50:1–16.
[38] Feo L, Luciano R, Misseri G, Rovero L. Irregular stone masonries: analysis and strengthening with glass fibre reinforced composites. Compos part b 2016;92: 84–93.
[39] Cavdar A. The effects of high temperature on mechanical properties of cementitious composites reinforced with polymer fibers. Compos part b 2013;45:78–88.
[40] Tosun-Felekoglu K, Felekoglu B. Effects of fiber-matrix interaction on multiple cracking performance of polymeric fiber reinforced cementitious composites. Compos part b 2013;52:62–71.
[41] Chung DDL. Functional materials. World Scientific Pub; 2010.

[42] http://scientificpolymer.com/density-of-polymers-by-density/.
[43] Riddle B, Baker-Jarvis J, Krupka J. Complex permittivity measurements of common plastics over variable temperatures. IEEE Trans Microw Theory Tech 2003;51:727–33.
[44] Ruan SQ, Jiang HW, Yin Y. Study on the influence of polypropylene fiber and SBR latex on the mechanical properties of rubber mortar and microstructures analyzed. Adv Mater Res (Durnten-Zurich, Switz) 2013;771(Materials in Industry and Nanotechnology):89–93.
[45] Wei J, Cheng F, Yuan H. Electrical resistance and microstructure of latex modified carbon fiber reinforced cement composites. J Wuhan Univ Technol Mater Sci Edi 2012;27(4):746–9.
[46] Pavlitschek T, Gretz M, Plank J. Effect of Ca^{2+} ions on the film formation of an anionic styrene/n-butylacrylate latex polymer in cement pore solution. Adv Mater Res (Durnten-Zurich, Switz) 2013;687:322–8.
[47] Sheng Q, Diamond S. SEM observations of latex networks in latex-modified concrete. Proc Int Conf Cem Microsc 1990;12:403–10.
[48] Wang R, Wang P. Microstructural aspects of SBR latex-modified cement paste and mortar highlighted by means of SEM and ESEM. Proc Int Conf Cem Microsc 2009. 31st:wang1/1-wang1/11.
[49] Shi X, Wang R, Wang P. Dispersion and absorption of SBR latex in the system of mono-dispersed cement particles in water. Adv Mat Res (Durnten-Zurich, Switz) 2013;687:347–53.
[50] Li J, Zhong S, Zhang C. Influence of superplasticiser and mixing procedure on properties of styrene-acrylic ester latex modified mortars. Mag Concr Res 2012;64(5):411–7.
[51] Rozenbaum O, Pellenq RJ, Van Damme H. An experimental and mesoscopic lattice simulation study of styrene-butadiene latex-cement composites properties. Mater Struct (Bagneux, Fr) 2005;38(278):467–78.
[52] Ramli M, Tabassi AA, Hoe KW. Porosity, pore structure and water absorption of polymer-modified mortars: an experimental study under different curing conditions. Compos part b 2013;55:221–33.
[53] Liu J, Xu C, Zhu X, Wang L. Modification of high performances of polymer cement concrete. J Wuhan Univ Technol Mater Sci Ed 2003;18(1):61–4.
[54] Kong X, Li Q. Properties and microstructure of polymer modified mortar based on different acrylate latexes. Guisuanyan Xuebao 2009;37(1):107–14.